CLINICAL ORAL IMPLANTS RESEARCH

Three-dimensional bone structure and bone mineral density evaluations of autogenous bone graft after sinus augmentation: a microcomputed tomography analysis

Journal:	*Clinical Oral Implants Research*
Manuscript ID:	Draft
Manuscript Type:	Original Research
Date Submitted by the Author:	n/a
Complete List of Authors:	Huang, Heng Li; China Medical University, School of Dentistry Chen, Michael YC; China Medical University Hospital, Dental Department Hsu, Jui-Ting; China Medical University, School of Dentistry Li, Yu-Fen; China Medical University, Graduate Institute of Biostatistics Chang, Ching-Han; National Cheng Kung University, Institute of Biomedical Engineering Chen, Kuan-Ting; China Medical University, Biostatistics Center
Keywords:	Bone substitutes, CT Imaging, Sinus floor elevation, Clinical research, Clinical trials

Three-dimensional bone structure and bone mineral density evaluations of autogenous bone graft after sinus augmentation: a microcomputed tomography analysis

Heng-Li Huang[1*], Michael YC Chang[1*], Jui-Ting Hsu[1], Yu-Fen Li[2,3], Ching-Han Chang[4] , Kuan-Ting Chen[3]

* indicates equal contribution

[1] School of Dentistry, China Medical University, 91 Hsueh-Shih Road, Taichung, Taiwan.

[2] Biostatistics Center, China Medical University, 91 Hsueh-Shih Road, Taichung 404, Taiwan.

[3] Graduate Institute of Biostatistics, China Medical University, 91 Hsueh-Shih Road, Taichung 404, Taiwan.

[4] Institute of Biomedical Engineering, National Cheng Kung University, Tainan, Taiwan.

Running title: Micro-CT analysis of autogenous bone graft

Corresponding Author: Heng-Li Huang. School of Dentistry, China Medical University, Taichung, Taiwan. Full Address: School of Dentistry, China Medical University, 91 Hsueh-Shih Road, 40402 Taichung, Taiwan. Fax: 1-886-4-22014043 Phone: 1-886-4-22053366 ext. 2307. E-mail: hlhuang@mail.cmu.edu.tw

Abstract: **Objective:** The purpose of this study was to determine the relationships and differences in three-dimensional (3D) bone mineral density (BMD) and microtrabecular structures between autogenous bone grafts and their adjacent native bone after a healing period following maxillary sinus augmentation. **Materials and Methods:** Ten rod-shaped human bone biopsy samples were harvested from patients receiving two-stage sinus augmentation therapy in implant placement areas, and analyzed by microcomputed tomography (micro-CT). Before micro-CT scanning, two BMD phantoms were placed near to the bone biopsy samples for executing BMD calculations of the grafted and native bone samples. In addition, 3D structural parameters of the trabeculae were analyzed for both the grafted and native bone, including percentage of bone volume [bone volume (BV)/tissue volume (TV)], bone-specific surface [bone surface (BS)/BV], trabecular thickness (Tb.Th), trabecular number (Tb.N), trabecular separation (Tb.Sp), trabecular pattern factor (Tb.Pf), and structure model index (SMI). **Results:** No significant correlations with regard to BMD and trabecular-structure parameters were found between native bone and grafted bone; however, BS/BV and Tb.Pf were higher and Tb.Th was 38% lower in grafted bone than in native bone. For grafted bone, there were significant correlations ($p < 0.05$) between BMD and BV/TV, Tb.Th, and Tb.Pf. **Conclusions:** When using autogenous bone as a graft material, the BMD and micromorphologic conditions of grafted bone were not influenced by the condition of the native bone in the maxilla. Differences were found in surface complexity, trabecular thickness, and the connectivity of trabeculae between grafted bone and native bone. The BMD in grafted bone was affected by the quantity and connectivity of the trabeculae.

Keywords: autogenous bone graft, sinus augmentation, micro-CT, bone mineral density, trabecular-structure parameters

Introduction

Dental implants have shown a high success rate (≥90%) (Eckert & Wollan 1998) in both the mandible and maxilla. However, due to insufficient bony support in the maxillary sinus cavity, the posterior maxilla represents a challenge for implant placement. A routine procedure for improving the prognosis of implant placement in the posterior maxilla is sinus augmentation (Armand et al. 2002, Chanavaz 2000). In this surgical procedure, a small window is shaped in the lateral wall of the maxilla, the sinus epithelium is elevated, and a space is created that is then filled with a grafting material. Since Boyne and James first demonstrated the usefulness of autogenous grafts in the sinus floor (Boyne & James 1980), autogenous bone has been used regularly for craniofacial bone grafting to accompany dental implant treatment (McAllister & Haghighat 2007).

While various graft materials have been developed (Garg 2004, Scarano et al. 2006), autogenous bone graft (in block or particulate form) remains a gold standard for sinus augmentation (Del Fabbro et al. 2004). Autogenous bone grafting provides a satisfactory source of osteogenic cells without the risk of antigenicity or crossinfection (Kaufman 2003). Its use is popular in the clinical setting due to its osteoconductive, osteoinductive, and osteogenic properties (Nkenke & Stelzle 2009). However, the volume of bone and the donor site than can be harvested are limited. The posterior iliac crest is the most commonly used donor site as it has the greatest amount of bone available – up to 140 ml is needed (Garg 2004).

Microcomputed tomography (micro-CT) is now widely used for observing and analyzing the internal structure of hard tissues because it is quick, reproducible, and nondestructive (Feldkamp et al. 1989). Many studies have used micro-CT to obtain high-resolution images and assess the trabecular structure of human bone quantitatively in three dimensions (Fanuscu & Chang 2004, Hildebrand et al. 1999, Muller et al. 1998). Interest in micro-CT in the field of dental implants is increasing; it is increasingly employed to evaluate peri-implant bone (Akca et al. 2006, Morinaga et al. 2009, Rebaudi et al. 2004, Sennerby et al. 2001), and has been validated using histomorphometric results (Cha et al. 2009, Park et al. 2005, Stoppie et al. 2005). This method also allows evaluation of the three-dimensional (3D) architecture of grafted bone after a period of bone healing (Chopra et al. 2009, Kon et al. 2009, Kuhl et al. 2010, Trisi et al. 2006). However, only few studies (Kon et al., 2009, Lee et al. 2007) have assessed the bone formation in autogenous bone grafts by micro-CT, and none of these studies has examined the differences in the 3D trabecular structure and bone mineral density (BMD) of autogenous bone grafts as compared to native bone after maxillary sinus augmentation.

The purpose of this study was to investigate the relationship between micro-CT measurement parameters describing BMD and 3D microtrabecular indexes (Table 1) in autogenous bone graft and its adjacent native bone after a healing period following maxillary sinus bone grafting. In addition, the relative effects of BMD and percentage of bone volume (BV; BV/tissue volume, TV) on the other trabecular-bone structures, including bone-specific surface [bone surface (BS)/BV] and trabecular thickness (Tb.Th)…etc were also evaluated.

Materials and Methods

Selection of patients

The cohort for this study comprised nine patients (five men and four women aged 44–61 years) who had undergone surgery to augment the maxillary sinus floor with autogenous bone grafts because of insufficient height of alveolar bone to allow dental implant placement. None of the patients had systemic pathologies affecting immune system functioning, non-insulin-dependent diabetes mellitus, or previous history of drug abuse. After being informed about the procedure, all of the patients gave written informed consent to participate in the study. The study protocol was approved by the Institutional Committee of China Medical University Hospital, Taichung, Taiwan (DMR96-IRB-180 & DMR97-IRB-260).

Bone biopsy preparation

After a 4- to 5-month period of autogenous bone graft healing and maturation, ten rod-shaped bone cores containing the native and grafted area of bone tissue were retrieved by trephine osteotomy (4.0 mm inner diameter) from the grafted site during surgical reentry for dental implant placement (Fig. 1). After removal, the biopsy samples were placed in 10% neutral buffered formalin solution.

Micro-CT scanning

A high-resolution, desktop, cone-Beam micro-CT system (SkyScan 1076, SkyScan, Aartselaar, Belgium) was used to quantify the BMD and other 3D microarchitecture parameters (Table 1). Before scanning, the bone biopsy samples were rinsed and stored in physiological saline solution (0.9%) within a polypropylene tube. X-ray source were set at 49 kV and 200 µA with the aid of a 0.5-mm-thick aluminum filter to optimize the contrast, a 360° rotation, a rotation step of 0.4° (2700 images per scan), three-frame averaging, and an exposure time of 1180 ms. The image resolution was fixed at a pixel size of 17.2 µm. During scanning, two BMD phantoms (SkyScan) that were 4.0 mm in diameter, 5.5 mm long, and had calcium hydroxyapatite densities of 0.25 and 0.75 g/cm^3 were placed near to the bone biopsy samples to aid BMD calculation.

NRecon reconstruction software (NRecon v.1.4.4, SkyScan) was used to create two-dimensional, 1000×1000-pixel images (Fig. 1). For the reconstruction parameters, ring artifact correction and smoothing were fixed at zero, and the beam hardening correction was set at 0%. Contrast limits were applied following SkyScan instructions. The lower limit was zero so that the density scale had a zero origin. The upper limit was at the top end of the brightness spectrum, representing the highest bone density value. After reconstruction, the volume of interest (VOI) was selected within the reconstructed images of water to calibrate the standard unit of X-ray computed tomography density (Hounsfield unit, HU) by using CTAn analysis software (v.1.6.0, SkyScan). A similar procedure was used to measure the HU values of two BMD phantom rods, followed by conversion from HU to BMD values (g/cm^3). Once the calibration of BMD against HU values was complete, the same VOI was applied to the images of the bone biopsy samples to calculate the BMD values of the grafted and native bone. The other 3D microtrabecular parameters (Table 1) were also analyzed for grafted bone and native bone by CTAn including BV/TV, BS/BV, Tb.Th, trabecular number (Tb.N), trabecular separation (Tb.Sp), trabecular pattern factor (Tb.Pf), and the structure model index (SMI).

Statistical and correlation analyses

All of the micro-CT measurement parameters are summarized as median values and interquartile ranges [25^{th}percentile (Q1)–75^{th} percentile (Q3)]. Comparisons of the parameters between native bone and grafted bone were analyzed with Wilcoxon's rank-sum test. The correlations among the parameters were performed using Spearman's rank correlation coefficient. All of the statistical analyses were executed using SAS software (SAS v9.2, SAS Institute, Cary, NC, USA). The level of statistical significance was set at α=0.05.

Results

Differences and correlations between the grafted and native bone parameters

Table 2 lists the median values and interquartile ranges of all measured parameters for the grafted and native bone. Significant differences between the two bone types were observed for only three of these parameters: BS/BV, Tb.Pf, and Tb.Th (p<0.05). BS/BV and Tb.Pf were higher for grafted bone [0.54 (1/pixel) and 0.18 (1/pixel), respectively] than for native bone [0.3 (1/pixel) and 0.08 (1/pixel), respectively]. The Tb.Th was 38% lower for the grafted bone (8.15 pixels) than for native bone (13.12 pixels). Correlations of these parameters between the grafted and native bone are shown in Fig. 2. Although the BMD and Tb.Th of the grafted bone were weakly positively correlated with those of native bone, the p value by Spearman's rank correlation test were not significant (p>0.05), indicating no predictable relationship regarding these parameters between the grafted and native bone.

Correlations of BMD and BV/TV with other trabecular-structure parameters

Regarding the native bone, no significant difference was shown between the BMD and the other trabecular-structure parameters (Table 3). However, for grafted bone, the BMD was significantly correlated with BV/TV (0.697), Tb.Th (0.733), and Tb.Pf (–0.648).

BV/TV was significantly correlated with BS/BV (–0.927), Tb.Th (0.903), Tb.N (0.903), and Tb.Sp (–0.915) in the native bone, but not with either Tb.Pf or SMI (Table 4). However, all of the parameters were strongly correlated (i.e., very significant) with BV/TV in the grafted bone (Table 3).

Discussion

X-ray examination is a common clinical method for evaluating the condition of grafted bone prior to dental implant placement. Even though this X-ray-based technique is noninvasive, it provides only low-resolution, two-dimensional images. Histology and histomorphometric techniques can be used to examine the bone mineral quality and trabecular-bone structure of grafted bone, but they can only provide one-time measurements that cannot be repeated on the same sample (Gedrange et al. 2005). In addition, only a few sections can be obtained by both X-ray and histomorphometric methods, and these two-dimensional images may not be representative of the entire specimen. The present study employed micro-CT and a 3D medical image processing system (Mimics software) to reconstruct and measure the precise 3D BMD and trabecular-structure indexes of grafted bone, in particular for maxillary sinus augmentation. This approach might provide more reliable information on how the autogenous bone graft transforms into the trabecular structure of grafted bone by quantifying both the BMD and the differences in BMD and morphological results between the grafted bone and its adjacent native bone.

The relationships between, and differences in BMD and other trabecular-structure indexes between grafted and native bone that were elucidated by micro-CT are important for two main reasons: to better understand the consequences of the mineralization and trabecular remodeling of autogenous bone graft, and for the prognosis of subsequent dental implant treatment in the grafted maxillary sinus. In the present study, no significant correlation ($p>0.05$) was found for any of the parameters between the grafted bone and its adjacent native bone (Fig. 2). This result implies that the condition of native bone in the atrophic maxilla is unlikely to influence the condition of the adjacent grafted bone. Therefore, clinically there is no need to be concerned about the condition of the native bone prior to maxillary sinus augmentation surgery if an increase in bone volume in the atrophic maxilla is necessary in patients requiring a longer implant (>7 mm) for improved implantation outcome (Hagi et al. 2004).

According to the 3D-reconstructed image of the bone biopsy material (upper panel in Fig. 2c), it is clear that the morphology of the trabecular structure of the grafted bone is different from that in native bone. The findings listed in Table 2 confirm this observation, and demonstrate that Tb.Th is significantly lower, and Tb.Pf and BS/BV are significantly higher in grafted bone than in native bone. This makes sense for the grafted bone, since trabeculae are thin (upper panel in Fig. 2b), and more disconnected trabecular bone may occur, resulting in highly complex trabecular structures. Since Tb.Th and Tb.Pf are indexes that reflect the status of the trabecular architecture, and both values are lower in grafted bone than in native bone from the atrophic maxilla, the immediate loading of an implant may not be an appropriate treatment following sinus augmentation. The lower stiffness of the grafted bone may increase the stress levels in the alveolar ridge around the implant (Huang et al. 2008).

Significant and strong correlations between BV/TV and BS/BV, Tb.Th, Tb.N, and Tb.Sp were found in native bone. The close relationship between BV/TV and trabecular structure is perhaps understandable, since with more thick and dense trabeculae, not only is the complexity of the trabecular structure reduced, but the BV/TV would be increased. Our results also suggest that the size and number of individual trabeculae are sensitive to the volume of the native bone present. That is, a loss of bone volume may affect the Tb.Th and Tb.N, resulting in a weak bone structure that is not suitable for dental or orthodontic implant placement.

With regard to the grafted bone, a positive relationship of BMD was observed with BV/TV, Tb.N, and Tb.Pf. This finding concurs with those of an animal study (Elsubeihi & Heersche 2004), in which it was reported that during healing following tooth extraction, the process of alveolar bone generation and remodeling resulted in a significant positive correlation between BMD and total BV. In the present study, strong correlations were also found between BV/TV and some indexes of trabecular structure (e.g., Tb.N and Tb.Pf). Therefore, calculating BMD of the grafted bone might also take into consideration the BV related to changes in the quantity (Tb.N) and connectivity (Tb.Pf) of the trabeculae, thus improving the likelihood of success of maxillary sinus augmentation.

One of the limitations of this study is the small sample. Even though our patient evaluation was objective, and patients were carefully assessed to ensure that they were without physiological disease, a larger sample is required to strengthen the statistical power. However, we do believe that the present findings are worthwhile, and can be regarded as a general principle and thus useful to clinicians. Furthermore, although autogenous bone is believed to be a gold standard for bone augmentation, there are some factors that may influence the bone remodeling and mineralization of autogenous bone grafts, for example gender, particle size (Kon et al., 2009), and location of the donor site (Gerressen et al. 2008, Klijn et al. 2010, Thorwarth et al. 2005). Therefore, further clinical studies are needed to elucidate the detailed mechanisms underlying the effect of these factors on the BMD and morphology of trabeculae.

Conclusions

Within the limitations of the present study, the following conclusions can be drawn:

1. In grafted bone, the surface complexity (i.e., BS/BV) and Tb.Th were higher, and the connectivity of trabeculae (i.e., Tb.Pf) was lower than in native bone.
2. No significant correlations with regard to BMD and trabecular structures were evident between the native and grafted bone. The clinical implication of this result may be that the condition of native bone in the atrophic maxilla would not influence the condition of its adjacent grafted bone if patients with poor maxillary bone quality need sinus augmentation prior to dental implant placement.
3. A positive correlation between BMD and BV/TV was found in grafted bone. An explanation for this relationship may be changes in the quantity and connectivity of the trabeculae.

Acknowledgement

This research was supported by National Science Council (NSC 98-2320-B-039-005-MY3), Taiwan.

Akca, K., Chang, T., Tekdemir & Fanuscu, M. (2006) Biomechanical aspects of initial intraosseous stability and implant design: A quantitative micro morphometric analysis. *Clinical Oral Implants Research* **17**: 465-472.

Armand, S., Kirsch, A., Sergent, C., Kemoun, P. & Brunel, G. (2002) Radiographic and histologic evaluation of a sinus augmentation with composite bone graft: A clinical case report. *Journal of Periodontology* **73**: 1082-1088.

Boyne, P. & James, R. (1980) Grafting of the maxillary sinus floor with autogenous marrow and bone. *Journal of Oral Surgery (American Dental Association: 1965)* **38**: 613.

Cha, J., Lim, J., Song, J., Sato, D., Kenmotsu, M., Inoue, T. & Park, Y. (2009) Influence of the length of the loading period after placement of orthodontic mini-implants on changes in bone histomorphology: Microcomputed tomographic and histologic analysis. *The International Journal of Oral & Maxillofacial Implants* **24**.

Chanavaz, M. (2000) Sinus graft procedures and implant dentistry: A review of 21 years of surgical experience (1979-2000). *Implant Dentistry* **9**: 197.

Chopra, P., Johnson, M., Nagy, T. & Lemons, J. (2009) Micro computed tomographic analysis of bone healing subsequent to graft placement. *Journal of Biomedical Materials Research Part B: Applied Biomaterials* **88**: 611-618.

Del Fabbro, M., Testori, T., Francetti, L. & Weinstein, R. (2004) Systematic review of survival rates for implants placed in the grafted maxillary sinus. *The International Journal of Periodontics & Restorative Dentistry* **24**: 565.

Eckert, S. & Wollan, P. (1998) Retrospective review of 1170 endosseous implants placed in partially edentulous jaws. *The Journal of Prosthetic Dentistry* **79**: 415-421.

Elsubeihi, E. & Heersche, J. (2004) Quantitative assessment of post-extraction healing and alveolar ridge remodelling of the mandible in female rats. *Archives of Oral*

Biology **49**: 401-412.

Fanuscu, M. & Chang, T. (2004) Three dimensional morphometric analysis of human cadaver bone: Microstructural data from maxilla and mandible. *Clinical Oral Implants Research* **15**: 213-218.

Feldkamp, L., Goldstein, S., Parfitt, M., Jesion, G. & Kleerekoper, M. (1989) The direct examination of three dimensional bone architecture in vitro by computed tomography. *Journal of Bone and Mineral Research* **4**: 3-11.

Garg, A. (2004) Bone biology, harvesting, and grafting for dental implants: Rationale and clinical applications: Quintessence Pub. Co.

Gedrange, T., Hietschold, V., Mai, R., Wolf, P., Nicklisch, M. & Harzer, W. (2005) An evaluation of resonance frequency analysis for the determination of the primary stability of orthodontic palatal implants. A study in human cadavers. *Clinical Oral Implants Research* **16**: 425-431.

Gerressen, M., Prescher, A., Riediger, D., Van Der Ven, D. & Ghassemi, A. (2008) Tibial versus iliac bone grafts: A comparative examination in 15 freshly preserved adult cadavers. *Clinical Oral Implants Research* **19**: 1270-1275.

Hagi, D., Deporter, D., Pilliar, R. & Arenovich, T. (2004) A targeted review of study outcomes with short (7 mm) endosseous dental implants placed in partially edentulous patients. *Journal of Periodontology* **75**: 798-804.

Hahn, M., Vogel, M., Pompesius-Kempa, M. & Delling, G. (1992) Trabecular bone pattern factor--a new parameter for simple quantification of bone microarchitecture. *Bone* **13**: 327-330.

Hildebrand, T., Laib, A., Muller, R., Dequeker, J. & Ruegsegger, P. (1999) Direct three dimensional morphometric analysis of human cancellous bone: Microstructural data from spine, femur, iliac crest, and calcaneus. *Journal of Bone and Mineral* *research* **14**: 1167-1174.

Hildebrand, T. & Ruegsegger, P. (1997) Quantification of bone microarchitecture with the structure model index. *Computer Methods in Biomechanics and Biomedical Engineering* **1**: 15-23.

Huang, H., Fuh, L., Hsu, J., Tu, M., Shen, Y. & Wu, C. (2008) Effects of implant surface roughness and stiffness of grafted bone on an immediately loaded maxillary implant: A 3d numerical analysis. *Journal of Oral Rehabilitation* **35**: 283-290.

Kaufman, E. (2003) Maxillary sinus elevation surgery: An overview. *Journal of Esthetic and Restorative Dentistry* **15**: 272-283.

Klijn, R., Meijer, G., Bronkhorst, E. & Jansen, J. (2010) Sinus floor augmentation surgery using autologous bone grafts from various donor sites: A meta-analysis of the total bone volume. *Tissue Engineering Part B: Reviews* **16**: 295-303.

Kon, K., Shiota, M., Ozeki, M., Yamashita, Y. & Kasugai, S. (2009) Bone augmentation ability of autogenous bone graft particles with different sizes: A histological and micro computed tomography study. *Clinical Oral Implants Research* **20**: 1240-1246.

Kuhl, S., Gotz, H., Hansen, T., Kreisler, M., Behneke, A., Heil, U., Duschner, H. & d'Hoedt, B. (2010) Three-dimensional analysis of bone formation after maxillary sinus augmentation by means of microcomputed tomography: A pilot study. *The International Journal of Oral & Maxillofacial Implants* **25**: 930.

Lee, S., Choi, B., Li, J., Jeong, S., Kim, H. & Ko, C. (2007) Comparison of corticocancellous block and particulate bone grafts in maxillary sinus floor augmentation for bone healing around dental implants. *Oral Surgery, Oral Medicine, Oral Pathology, Oral Radiology, and Endodontology* **104**: 324-328.

McAllister, B. & Haghighat, K. (2007) Bone augmentation techniques. *Journal of*

Periodontology **78**: 377-396.

Morinaga, K., Kido, H., Sato, A., Watazu, A. & Matsuura, M. (2009) Chronological changes in the ultrastructure of titanium bone interfaces: Analysis by light microscopy, transmission electron microscopy, and micro computed tomography. *Clinical Implant Dentistry & Related Research* **11**: 59-68.

Muller, R., Van Campenhout, H., Van Damme, B., Van Der Perre, G., Dequeker, J., Hildebrand, T. & Ruegsegger, P. (1998) Morphometric analysis of human bone biopsies: A quantitative structural comparison of histological sections and micro-computed tomography. *Bone* **23**: 59-66.

Nkenke, E. & Stelzle, F. (2009) Clinical outcomes of sinus floor augmentation for implant placement using autogenous bone or bone substitutes: A systematic review. *Clinical Oral Implants Research* **20**: 124-133.

Park, Y., Yi, K., Lee, I. & Jung, Y. (2005) Correlation between microtomography and histomorphometry for assessment of implant osseointegration. *Clinical Oral Implants Research* **16**: 156-160.

Rebaudi, A., Koller, B., Laib, A. & Trisi, P. (2004) Microcomputed tomographic analysis of the peri-implant bone. *The International Journal of Periodontics & Restorative Dentistry* **24**: 316.

Scarano, A., Degidi, M., Iezzi, G., Pecora, G., Piattelli, M., Orsini, G., Caputi, S., Perrotti, V., Mangano, C. & Piattelli, A. (2006) Maxillary sinus augmentation with different biomaterials: A comparative histologic and histomorphometric study in man. *Implant Dentistry* **15**: 197.

Sennerby, L., Wennerberg, A. & Pasop, F. (2001) A new microtomographic technique for non invasive evaluation of the bone structure around implants. *Clinical Oral Implants Research* **12**: 91-94.

Stoppie, N., Waerden, J., Jansen, J., Duyck, J., Wevers, M. & Naert, I. (2005) Validation of microfocus computed tomography in the evaluation of bone implant specimens. *Clinical Implant Dentistry & Related Research* **7**: 87-94.

Thorwarth, M., Srour, S., Felszeghy, E., Kessler, P., Schultze-Mosgau, S. & Schlegel, K. (2005) Stability of autogenous bone grafts after sinus lift procedures: A comparative study between anterior and posterior aspects of the iliac crest and an intraoral donor site. *Oral Surgery, Oral Medicine, Oral Pathology, Oral Radiology, and Endodontology* **100**: 278-284.

Trisi, P., Rebaudi, A., Calvari, F. & Lazzara, R. (2006) Sinus graft with biogran, autogenous bone, and prp: A report of three cases with histology and micro-ct. *The International Journal of Periodontics & Restorative Dentistry* **26**: 113.

Fig. 1. Grafted bone biopsy sample obtained using a 4.0-mm (inner diameter) trephine bur.

Fig. 2. Two-dimensional X-ray image of the grafted bone biopsy sample (a) and its two-dimensionally reconstructed images which were used to set the region of interest (ROI) in the grafted (upper) and native (lower) bone (b), were used to create a three-dimensional (3D) construction model (upper) for trabecular-structure analysis and for 3D bone mineral density (BMD) evaluation by comparison with BMD phantoms of 0.25 and 0.75 g/cm^3 (lower) (c).

Fig. 3. Distribution plots for BMD (a), percentage of bone [i.e., bone volume (BV)/tissue volume (TV)] (b), bone-specific surface [bone surface (BS)/BV] (c), trabecular bone thickness (Tb.Th) (d), trabecular number (Tb.N) (e), trabecular pattern factor (Tb.Pf) (f), structure model index (SMI) (g), and trabecular separation (Tb.Sp) (h) of native bone in relation to those of grafted bone on each bone biopsy specimen. Correlations and *p* values were analyzed by Spearman's rank correlation test.

Table 1. Brief definitions of the parameters of microcomputed tomography (micro-CT) analysis in the present study (note: 1 pixel = 17.2 μm)

Parameter	Abbreviation (Unit)	Definition
Bone mineral density	BMD (g/cm^3)	The volumetric density of calcium hydroxyapatite (in g/cm^3). It is calibrated with the aid of phantoms with known BMDs.
Percentage of bone volume	BV/TV (%)	Percentage of bone volume (BV) relative to tissue volume (TV) within a volume of interest (VOI).
Bone-specific surface	BS/BV (1/pixel)	Ratio of bone surface (BS) to BV; this is a useful basic index for characterizing the complexity of structures.
Trabecular thickness	Tb.Th (pixel)	Mean thickness of individual trabecular bones within a VOI.
Trabecular number	Tb.N (1/pixel)	The number of traversals across a trabecular bone per unit length on a linear path within a VOI.
Trabecular separation	Tb.Sp (pixel)	Relative spacing between individual trabecular bones within a VOI.
Trabecular pattern factor	Tb.Pf (1/pixel)	An index of the connectivity of trabecular bone, which was developed by Hahn et al. in 1992 (Hahn et al. 1992). A lower Tb.Pf signifies better-connected trabecular lattices, while a higher Tb.Pf indicates a more disconnected trabecular structure.
Structure model index	SMI (none)	This relative index was derived according to the method of Hildebrand and Ruegsegger in 1997 (Hildebrand & Ruegsegger 1997). It is used to characterize trabecular bone according to its transition from plate-like to rod-like architecture. An ideal plate and cylinder have SMI values of 0 and 3, respectively.

Table 2. The median (interquartile range) values of micro-CT measurement parameters of native bone and grafted bone.

Parameters	Native bone (n=10)	Grafted bone (n=10)	*P*-value
BMD	0.26(0.08-0.44)	0.14(0.07-0.34)	0.521
BV/TV	27.37(18.65-45.79)	15.43(12.64-27.89)	0.089
BS/BV	0.30(0.22-0.38)	0.54(0.42-0.60)	0.004
Tb.Th	13.12(10.88-18.90)	8.15(7.46-10.59)	0.007
Tb.N	0.02(0.02-0.02)	0.02(0.01-0.03)	0.734
Tb.Pf	0.08(0.04-0.09)	0.18(0.05-0.26)	0.038
SMI	1.74(1.54-1.87)	2.30(1.66-2.43)	0.162
Tb.Sp	29.33(24.22-35.01)	25.37(20.62-27.74)	0.064

Median(interquartile range), compared by Wilcoxon's rank-sum test.

Table 3. Comparison of BMD and BV/TV with the other parameters in grafted bone and native bone.

		BMD	BV/TV	BS/BV	Tb.Th	Tb.N	Tb.Pf	SMI	Tb.Sp
Native bone									
	BMD	1.000	0.564	-0.600	0.612	0.467	-0.370	-0.055	-0.515
	BV/TV		1.000	-0.927***	0.903***	0.903***	-0.479	-0.442	-0.915***
Grafted bone									
	BMD	1.000	0.697*	-0.539	0.588	0.733*	-0.648*	-0.467	-0.564
	BV/TV		1.000	-0.842**	0.794**	0.939***	-0.952***	-0.879***	-0.758*

Values are Spearman's rank correlation coefficients.

*$P < 0.05$, **$P < 0.01$, ***$P < 0.001$

Fig. 1. Grafted bone biopsy sample obtained using a 4.0-mm (inner diameter) trephine bur.
244x174mm (72 x 72 DPI)

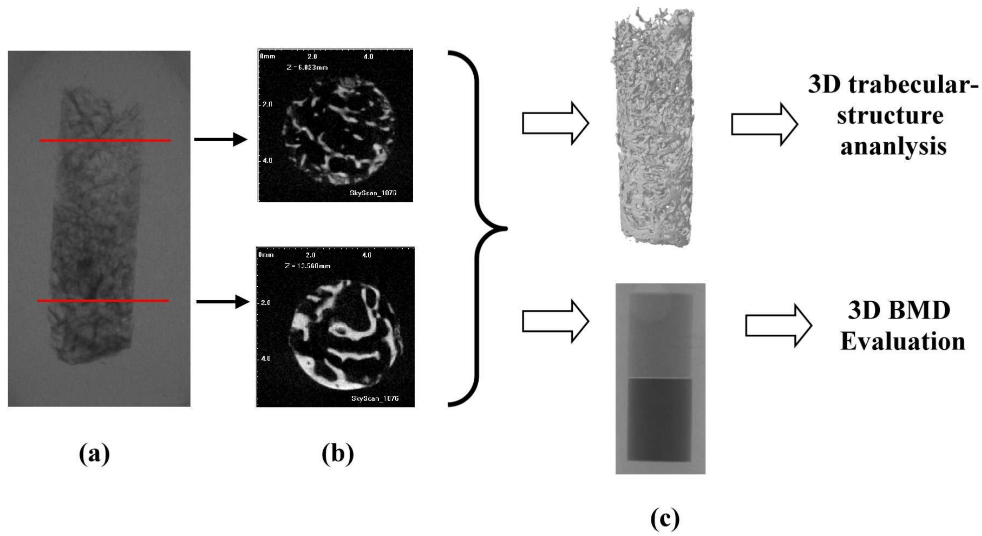

Fig. 2. Two-dimensional X-ray image of the grafted bone biopsy sample (a) and its two-dimensionally reconstructed images which were used to set the region of interest (ROI) in the grafted (upper) and native (lower) bone (b), were used to create a three-dimensional (3D) construction model (upper) for trabecular-structure analysis and for 3D bone mineral density (BMD) evaluation by comparison with BMD phantoms of 0.25 and 0.75 g/cm3 (lower) (c).
652x378mm (72 x 72 DPI)

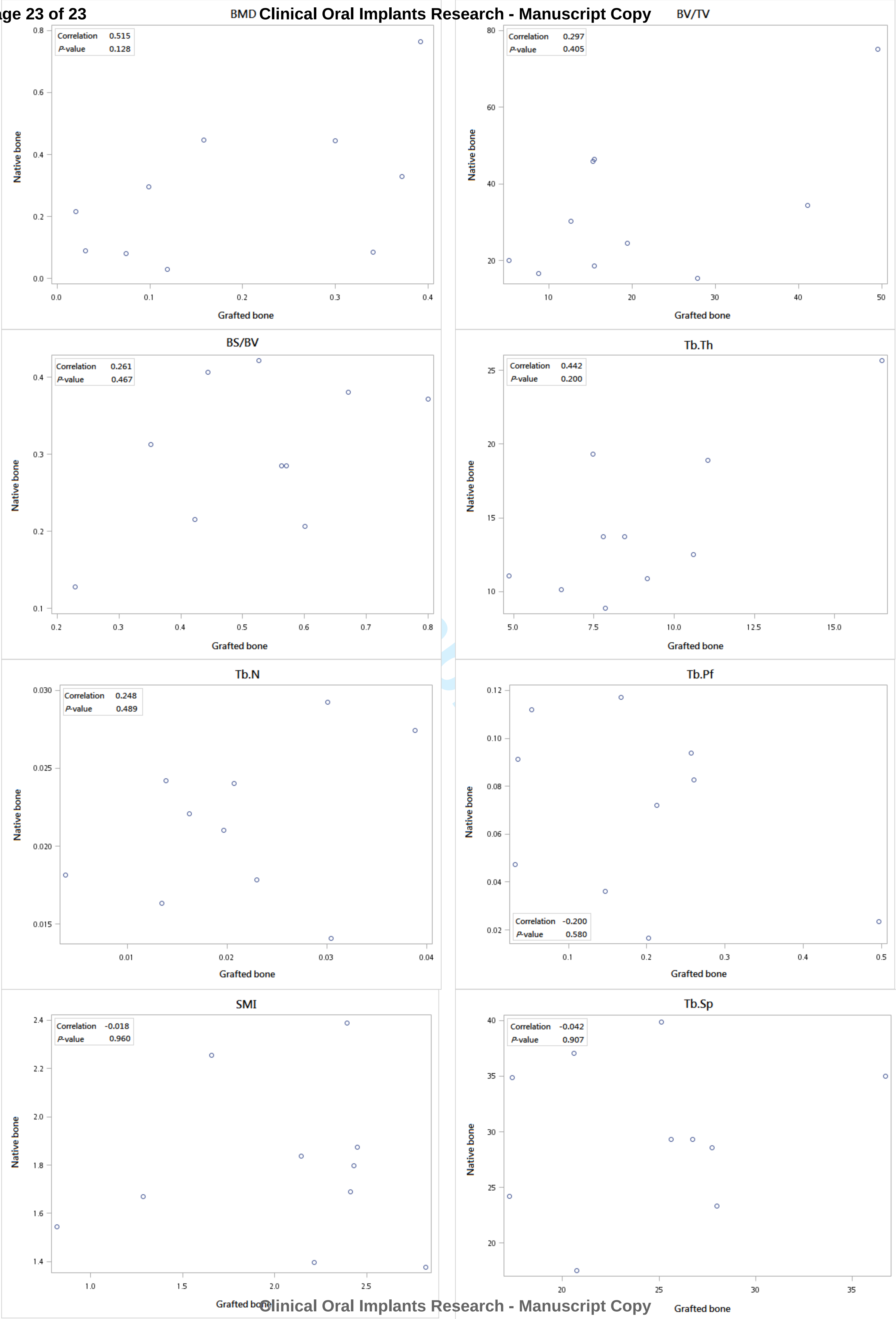
BMD
Correlation 0.515
P-value 0.128
Native bone
Grafted bone
BV/TV
Correlation 0.297
P-value 0.405
Native bone
Grafted bone
BS/BV
Correlation 0.261
P-value 0.467
Native bone
Grafted bone
Tb.Th
Correlation 0.442
P-value 0.200
Native bone
Grafted bone
Tb.N
Correlation 0.248
P-value 0.489
Native bone
Grafted bone
Tb.Pf
Correlation -0.200
P-value 0.580
Native bone
Grafted bone
SMI
Correlation -0.018
P-value 0.960
Native bone
Grafted bone
Tb.Sp
Correlation -0.042
P-value 0.907
Native bone
Grafted bone